NASA Technical Memorandum 84485

NASA-TM-84485 19820017340

THIS ROOM

SUBSONIC AERODYNAMIC AND FLUTTER CHARACTERISTICS OF SEVERAL WINGS CALCULATED BY THE SOUSSA P1.1 PANEL METHOD

E. CARSON YATES, JR., HERBERT J. CUNNINGHAM,
ROBERT N. DESMARAIS, WALTER A. SILVA, AND
BOHDAN DROBENKO

MAY 1982

LIBRARY COPY

MAY 25 1982

LANGLEY RESEARCH CENTER
LIBRARY, NASA
HAMPTON, VIRGINIA

NASA
National Aeronautics and
Space Administration

Langley Research Center
Hampton, Virginia 23665

SUBSONIC AERODYNAMIC AND FLUTTER CHARACTERISTICS OF SEVERAL WINGS CALCULATED BY THE SOUSSA P1.1 PANEL METHOD

E. Carson Yates, Jr., Herbert J. Cunningham, Robert N. Desmarais
Walter A. Silva,* and Bohdan Drobenko**
NASA Langley Research Center
Hampton, Virginia 23665

Abstract

The SOUSSA (Steady, Oscillatory, and Unsteady Subsonic and Supersonic Aerodynamics) program is the computational implementation of a general potential-flow analysis (by the Green's function method) that can generate pressure distributions on complete aircraft having arbitrary shapes, motions, and deformations. This paper presents results of some applications of the initial release version of this program to several wings in steady and oscillatory motion, including flutter. The results are validated by comparisons with other calculations and experiments. Experiences in using the program as well as some recent improvements are described.

Nomenclature

A_{ij}	generalized aerodynamic force
b	wing root semichord
C_{L_α}	lift-curve slope
C_p	pressure coefficient
ΔC_p	lifting-pressure coefficient, $C_{p_\ell} - C_{p_u}$
k	reduced frequency, $\frac{b\omega}{V}$
M	freestream Mach number
N_p	total number of panels on one-quarter of wing surface, e.g., on upper right-hand side
R	Reynolds number based on average chord
V	freestream speed
x	local chordwise coordinate measured from leading edge, fraction of local chord
x_L	fuselage longitudinal coordinate measured from nose, fraction of fuselage length
y	spanwise coordinate, fraction of semispan
Re,Im	real part, imaginary part
α	angle of attack
μ	mass ratio, mass of wing divided by mass of a volume of air at freestream density contained within a cylinder circumscribed about wing planform
ω	circular frequency of wing oscillation
ω_α	circular frequency of first torsion mode

Subscripts:

u,ℓ	upper surface, lower surface

Introduction

Application of a generalized Green's function method to the full, time-dependent potential-flow equation leads to an integral equation for the velocity potential at any point in the flow, including points on the surface of a body or bodies in the flow.[1,2] The SOUSSA (Steady, Oscillatory, and Unsteady Subsonic and Supersonic Aerodynamics) P1.1* computer program[3,4] is a panel-method code which implements this integral equation for linearized subsonic flow in the complex-frequency domain, and within that context is applicable to general shapes such as complete aircraft or other bodies having aribitrary shapes, motions, and deformations. A program with this degree of generality has many possible uses, including (1) unsteady-state applications, such as flutter, gust-response, and active-controls analyses with multiple sets of frequencies, mode shapes, and Mach numbers, and (2) steady or quasi-steady state applications such as aerodynamic analyses requiring pressure distributions and aerodynamic coefficients, static or dynamic stability analyses requiring stability derivatives (including rate derivatives), static aeroelastic analyses, and structural load calculations. The purpose of this paper is to present the results of some applications of SOUSSA P1.1 to several wings in both steady and oscillatory motion, including flutter, to validate the results by comparisons with other calculations and experiments, and to describe experiences in using the program as well as some recent improvements made to it.

The SOUSSA panel method was not formulated primarily for application to isolated wings of simple shape, nor was it intended to be a competitor of lifting-surface theory. However, for validation purposes the present study focuses on pressure-distribution and flutter calculations for such simple shapes so that comparisons can be made with both steady and unsteady lifting-surface calculations as well as with existing experimental data. Accordingly, the present study includes aerodynamic calculations for two rectangular wings,[5] a clipped-tip delta wing,[6] and two swept wings. Calculations were made for one of the swept wings with and without a fuselage.[7] Steady and unsteady pressure distributions are compared with experiments and with other calculations made with lifting-surface theory.[8-10] Flutter calculations are included for four rectangular wings which are essentially identical except for wing thickness. The resulting flutter characteristics are compared with those obtained by use of lifting-surface theory[11] and with experimental data.[12] In all of the calculations, the number and distribution of panels has been varied in order to examine convergence of the results.

---

*Graduate Student, Boston University

**Graduate Student, Stanford University

*"P1.1" designates the first version of the program released through COSMIC, University of Georgia, Athens, GA.

SOUSSA Panel Method

Description

The analysis which the SOUSSA program implements is based on application of the infinite-space Green's function method to the fully unsteady linearized velocity-potential partial differential equation.[1] The result is an integral expression for the velocity potential at any point in the flow at any time in terms of the value of the potential and its normal derivative over the surface of the body and its wake. If the field point lies on the surface of the body, the expression becomes an integro-differential delay equation for the potential on the surface of the body. Computation of the integral over the surface of the body is accomplished by surface paneling with twisted quadrilateral (hyperboloidal) panels which maintain continuity of the surface, although discontinuities in surface slope are introduced.[13] The result is a set of differential-delay equations in time. The time integration can be accomplished directly in the time domain by finite-difference procedures.However, the P1.1 version of the program[3,4] employs a Laplace-transform solution which yields frequency-domain (complex frequency) aerodynamics in the form of a matrix equation relating the velocity potential (usually unknown) to the normalwash distribution (usually known from specified shape, motion, and deformation of the body). Premultiplying the matrix equation by a matrix relating surface pressures or generalized forces to the potential and postmultiplying by a matrix relating the normalwash to the generalized coordinates permits direct calculation of surface pressures or generalized forces (weighted integrals of pressure).

The surface boundary condition implicit in the SOUSSA formulation is equivalent to the usual no-penetration condition and is automatically satisifed by the representation obtained from the Green's theorem. As a consequence, the perturbation potential is zero inside the body so that disturbances do not propagate into the interior. The far-field boundary condition is automatically satisifed by the source and doublet singularities distributed over the body and wake surfaces.

In the SOUSSA P1.1 code, the velocity potential is taken to be constant over each of the quadrilateral panels (zeroth-order panels). Although higher-order panels have been formulated for both subsonic and supersonic speeds, they have not yet been implemented in the program. The wake in the P1.1 program is assumed to have zero thickness and to extend downstream approximately in the freestram dirction. It is not required to be flat, but its shape remains "frozen" during the calculations.

The SOUSSA P1.1 program structure[3,4] is modular to facilitate inclusion of new capabilities or improved algorithms and to provide restart capability. Conservation of computer memory is emphasized to permit application to complicated shapes, such as complete aircraft, requiring large numbers of panels. Efficient computations are possible for multiple frequencies and/or multiple sets of vibration or deformation modes because the aerodynamic influence-coefficient integrals are independent of both mode shape and frequency and because the elements of the influence matrix depend on frequency in a very simple way.

The P1.1 code employs the data base and data-handling utilities of the SPAR finite-element structural analysis program.[14] These were incorporated because SOUSSA P1.1 was originally intended for the calculation of steady-state structural loads and unsteady aerodynamics for flutter and gust-response calculation in multidisciplinary structural-optimization computations employing the SPAR structural analysis. The SPAR components, however, are unnecessary for stand-alone use. More efficient methods for stand-alone operation are available.

SOUSSA P1.1 does not have a built-in geometry preprocessor because it is considered preferable for the user to have the flexibility of choosing a geometry processor that is appropriate for his needs.

Program Improvements

Subsequent to the completion of the initial form of the SOUSSA P1.1 code and the publication of references 3 and 4, several significant improvements have been incorporated and others are known to be needed for any future version of the program. Among the latter, higher-order panels and elimination of SPAR components have already been mentioned. Another is transposition and revision of the solution algorithm to substantially reduce input/output (I/O) operations. In the application of steady- or unsteady-flow panel methods, such as PAN AIR[15,16] and SOUSSA, to large problems (hundreds of panels), the major part of the cost is I/O related. Preliminary considerations, based on operations count, indicate that reduction of I/O operations by transposition, along with the other changes mentioned, could reduce the cost of large SOUSSA calculations by nearly an order of magnitude relative to that for the current version of the P1.1 program. Improvements already made have reduced the cost of calculations by 35 to 50 percent relative to that for the initial version.

Some program modifications already or currently being accomplished are described in the following subsections.

Out-of-Core Solver - The computers usually used to implement SOUSSA, such as CDC CYBER 170 series machines, have a usable central memory of about 120,000 (decimal) words. When allowance is made for the essential code to solve the SOUSSA system of algebraic equations relating the values of the potential at the panel centers to the matrix containing the normalwash vectors, the largest complex matrix that can be stored in memory is about 250x250. This means, for example, that a wing with unsymmetric loading on the upper and lower surfaces could not be paneled finer than 11x11 panels on each surface,and complicated wing/body configurations could not be solved in core.

This limitation was overcome by writing an out-of-core solver to solve the system of simultaneous algebraic equations by LU decomposition. That is, the coefficient matrix, which is dense, nonsymmetrical, and complex, is factored into a unit upper triangular matrix U and a lower triangular matrix L. These matrices are stored on disk and the simpler triangular systems of equations are solved for each vibration mode of the problem. The disk files that are used to hold the original matrix and the factored matrix, as the latter is created, are both serial files so all file positioning is done with reads, rewinds, and backspaces, rather than with disk random accesses. This has two advantages, it makes the code very portable, and it makes it easy to estimate I/O efficiency by merely counting rewinds and backspaces. A drawback of this method is that it is slightly less efficient than disk random access.

It is very easy to compute the spectral norm condition number of the L and U matrices while performing an LU factorization. The condition number of the solution process is the product of these condition numbers and is a measure of the amount of error induced by the method used to solve the system of simultaneous equations. For all cases studied, this was not a significant source of error.

The out-of-core solver was developed expressly to permit the use of paneling schemes that lead to coefficient matrices too large to fit in memory. However, it was found that use of the out-of-core solver utilizing a small workspace reduces the execution cost of SOUSSA P1.1 calculations even when only a moderate number of panels are used. The reason for this is that the typical computer costing algorithm contains a term proportional to the product of central processor time and central memory space, and the time in this term is the time of the entire SOUSSA run.

Kutta Condition - One improvement needed but not yet incorporated is related to the Kutta condition. The usual requirement of pressure continuity across the wake is imposed in the calculation of the velocity potential. However, the use of constant-potential panels in SOUSSA P1.1 prevents accurate direct calculation of surface pressures near the trailing edge. The present program therefore imposes two conditions on the variation of pressure in that region from which upper- and lower-surface pressures can be evaluated near the trailing edge (See equations (5-22) to (5-28) of reference 3.): 1)The difference between upper- and lower-surface pressures is required to vanish as the square root of the distance from the trailing edge--a condition consistent with lifting-surface theory. 2)The average of upper- and lower-surface pressures at the trailing edge is taken to be the same as the average at the centers of the upper- and lower-surface panels adjacent to the trailing edge. The first of these conditions is reasonable as long as the airfoil tail angle is not large. As will be shown later in this paper, however, the second condition is not a good approximation and should be replaced by a better extrapolation or preferably by special trailing-edge panels. This condition was never thought to be an accurate characterization of pressure behavior near the trailing edge, but it was incorporated into this first computer implementation as a matter of expediency.

Analytic Wake Integration - The SOUSSA P1.1 program, as originally coded, used a paneling scheme for the wake similar to that for the body. It was soon found that for the range of reduced frequencies of practical interest, the wake would have to be paneled for as many as five chord lengths downstream. Also it was found that large variations in panel size degrades the numerical accuracy of the current version of SOUSSA, because it uses low-order elements. This means that the foremost wake panels cannot be larger than the panels at the trailing edge of the lifting surface. As a consequence it was often necessary to use more panels for the wake than for the oscillating lifting surface. Although the computation required for the wake panels is simple, the I/O service required places the same demand on the computer for the wake as it does for the lifting surfaces. This is a major part of the execution cost of SOUSSA P1.1. This problem was eased by paneling each wake strip with a single panel, extending to infinity, and integrating the interaction function analytically in the stream direction. In effect, this replaced a large number of low-order finite elements on each wake strip by a single high-order element on which disturbances propagate downstream with free-stream velocity as a consequence of the requirement that the pressure difference across the wake vanish. The streamwise integral over the wake is then the same incomplete modified Struve function that occurs as part of the unsteady kernel of the familiar potential-flow downwash integral equation[17] and can be evaluated by methods developed for that purpose. The particular method used for SOUSSA was the 24-term exponential approximation described in reference 18. In addition to integrating the wake interaction function in the stream direction, it also has to be integrated in the cross-stream direction. For the paneled wake this integration was performed in closed form. However, after performing the streamwise integration analytically, the cross-stream integrand is not integrable in closed form, so a Legendre-Gauss quadrature formula is used. By varying the quadrature order it was found that a very high order was needed for convergence. This is due to a singularity in the complex plane that is near the interval of integration for wing panels near the trailing edge.

The strongest part of this near singularity occurs in the zeroth-order (steady-flow) term. When the cross-stream wake integrand is expanded in powers of the frequency, all the terms that do not contain the logarithm of the frequency can be integrated in closed form. However, only the zeroth and first-power terms were integrated in closed form. The Legendre-Gauss quadrature was used to integrate only the difference between the cross-stream integrand and the zeroth and first-power terms of its expansion. This can be integrated accurately with a very low order quadrature. In SOUSSA P1.1 a four-point cross-span quadrature is used over each wake strip. Even though this technique of performing the spanwise integration is required only for wing panels near the trailing edge, the integrations are performed the same for all wake integrals to simplify the program.

Replacing a paneled wake by an analytic wake in this manner does not save much CPU (central processor unit) time. However, there is a very significant saving in I/O cost, memory cost, and CPU cost for I/O service. A typical SOUSSA P1.1 run with the analytical wake costs about half as much as the same run with an adequately paneled wake.

There are times when the analytical wake cannot be used, for example, if there is another lifting surface in the wake. For this reason the capability of using the paneled wake was left in the program as an option. All of the present calculations, however, employed the analytical wake integration.

Evaluation of generalized aerodynamic forces - Another improvement of the SOUSSA P1.1 code that is being developed is more accurate calculation of generalized aerodynamic forces. After the pressures have been calculated at the panel centers, the generalized aerodynamic forces (weighted integrals of pressure) are currently evaluated by multiplying each value of pressure by the associated panel area and by the value of the weight function (generalized-force mode) at the panel center and summing these products for all the panels. This process amounts to rectangular integration. As will be shown later in this paper, it can yield generalized aerodynamic forces that converge more slowly (with respect to number of panels) than most of the component pressures used in their evaluation. Clearly, a better integration scheme is needed. A subprogram to perform the integration by Gaussian quadrature (weighted or unweighted as required) has been written and is being debugged but has not been incorporated into SOUSSA P1.1.

An alternate revision that is being considered is integration by parts to permit evaluation of generalized aerodynamic forces directly from the potential.

Applications and Results

Aerodynamic Calculations

The SOUSSA P1.1 code calculates pressures at the centers of the surface panels. Since these points usually will not be located at spanwise stations where experimental data are available for comparison, it is necessary to interpolate the calculated pressure to theappropriate stations. In this study, the cubic spline was used for the spanwise interpolation.

In the following discussion statements of SOUSSA paneling arrays refer to the number of panels on one-quarter of the wing surface, e.g., the upper right-hand side. A 14-by-22 array, for example, indicates 14 panels from leading edge to trailing edge and 22 panels from root to tip. The left/right symmetry option in SOUSSA was used throughout. Since all of the configurations in this study are vertically symmetric (that is, symmetric with respect to the x-y plane), the vertical symmetry option of SOUSSA was used for calculations at zero angle of attack. Thus for a 14-by-22 array of panels, the number of unknowns (and hence the order of the matrix problem to be solved) is 308 for zero angle of attack and 616 for nonzero angle of attack. Note that the wake does not introduce additional unknowns into the problem.

Comparison of Pressure Distributions from SOUSSA P1.1 and RHOIV - An initial step in evaluating the accuracy of results from the SOUSSA P1.1 program is to compare distributions of pressure for thin, isolated wings as obtained from SOUSSA with values generated by a state-of-the-art lifting-surface method such as RHOIV[8,9]. Both steady and unsteady pressures for this purpose have been generated for a rectangular wing of aspect ratio 2.0, and a 45-degree swept wing generated by shearing back the rectangular one. Both wings have a one-percent thick biconvex airfoil. The motion is unit-amplitude pitch about an axis through the root-trailing-edge point. The Mach number is 0.9, and the two reduced frequencies are k = 0.0 and 0.3. These conditions and the rectangular-wing planform were chosen to provide continuity with some paneling-convergence results presented in figure 29 and 30 of reference 10.

For the SOUSSA calculations the half span of each wing was divided into a 10-by-10 array of panels (Figs. 1 and 2) spaced uniformly chordwise, and spaced spanwise in equal increments of an angular coordinate defined as the inverse cosine of fraction of semispan measured from the wing root. This latter distribution is called a "cosine distribution."

The program RHOIV, which implements the subsonic kernel-function lifting-surface theory, employs a series of lifting-pressure functions that are continuous over the wing except at edge and hingeline discontinuities, and effects a solution by downwash collocation. In the present calculations, 12 collocation points were used chordwise at each of 10 span stations.The resulting continuous pressure distributions can be evaluated everywhere except at discontinuities. The RHOIV calculations do not account for the one-percent wing thickness.

For the rectangular wing, figures 1(a) and (b) show the chordwise distribution of lifting pressure coefficient ΔC_p per radian of pitch amplitude at the 57.5 percent span station for the two frequencies. In figure 1(a) the pressure for k=0.0 agree very well except at the center of the foremost panel. Such a discrepancy is not unexpected where a small number of low-order panels (i.e., constant velocity potential on each panel) are used in regions where potential and pressure are varying rapidly. In figure 1(b) for k=0.3, the agreement of the real-part pressure is about the same as for k=0.0. For the imaginary-part pressures, the SOUSSA results are systematically slightly larger than the RHOIV results except at the most forward panel.

For the 45-degree-swept wing, the same 10-by-10 paneling was retained along with the pitch axis through the root trailing edge, and pressure distributions are shown in figures 2(a) and (b) for the same 57.5 percent span station. As can be seen, the differences between the SOUSSA and RHOIV pressures are somewhat larger than for the unswept wing.

The observed differences between SOUSSA and RHOIV pressures are attributable to two factors: (i) wing thickness effects in SOUSSA but not in RHOIV; and (ii) SOUSSA results near the leading edge are probably not fully conveged with respect to the number of panels used. Thickness effects on lifting pressure are probably very small here because the thickness ratio is only one percent. With regard to paneling convergence, figure 3 of reference 19 shows relevant steady-state pressure for a two-dimensional airfoil calculated by a zeroth-order panel method which for these conditions is comparable to SOUSSA P1.1. The results show that eight panels chordwise were sufficient to converge pressures over most of the airfoil surface but gave pressures that were higher than converged values near the leading edge. Those results are consistent with the SOUSSA/RHOIV comparisons in figures 1(a) and 2(a). Paneling convergence for SOUSSA results is illustrated and discussed later in this paper. (See also Ref. 10).

Rectangular Wing - Steady and unsteady pressure distributions have been calculated by SOUSSA P1.1 for an aspect-ratio 3 rectangular wing with a five-percent-thick circular-arc airfoil for which experimental pressure data are available in reference 5. Figure 3 shows the wing and the three stations at which pressures were measured. These stations are at approximately 50, 70, and 90 percent of semispan. Two paneling arrays were used in the calculations, 10 by 10 and 14 by 22. In both arrays the panels were uniformly distributed in both directions. The steady-state results are compared with measured pressures for two angles of attack at $M = 0.7$ in figure 4. As the figures show, the SOUSSA results for the two paneling arrays are essentially the same except for small differences near the wing edges and tip where the larger array is expected to resolve the pressures more accurately.

For zero angle of attack (Fig. 4(a)), the calculated variations of pressure are in qualitative agreement with experiment, but calculated pressure levels are consistently lower than experiment. Some of this difference may be caused by an effective increase in the model thickness due to the boundary layer. The agreement between calculated and measured pressures is, in fact, slightly better at $M = 0.7$ for which the Reynolds number is 4.0×10^6 and the boundary layer is assumed to be thinner than at $M = 0.24$, for which the Reynolds number is 2.2×10^6 (results not shown). The experimental data, however, show no evidence of flow separation. Even though the pressures calculated by SOUSSA P1.1 are not in very close agreement with experiment, they are in very good agreement, over the interior portion of the planform, with those obtained from LTRAN3, a finite-difference small-perturbation potential-flow code[20] (comparison not shown).

At five degrees angle of attack figure 4(b) shows SOUSSA pressures to be in reasonable agreement with experimental values except near the sharp leading edge where the broad region of high suction in the measured upper-surface pressures shows evidence of a separation bubble. Also, just ahead of the trailing edge the calculated pressures (especially those obtained with the larger number of panels) level off, that is, deviate from the general downward trend, as a result of the inadequate implementation of the trailing-edge condition discussed previously.

The unsteady pressures in figure 5 were measured and calculated for the wing oscillating in its first bending mode. A 10-by-10 uniform array of panels was used in the SOUSSA calculations because the steady-state results (Fig. 4) showed that to be sufficient to obtain reasonably converged pressures. The resulting surface pressures (Fig. 5) are in good agreement with the scattered experimental values and with values calculated by the kernel-function lifting-surface theory.

Clipped-Tip Delta Wing - The clipped-tip delta wing shown in figure 6 is the one used in the experimental investigation of reference 6. All of the data presented in reference 6 are for Mach number 0.9; however, all of the data for this wing shown herein are for Mach number 0.4. Both sets of data were acquired during the same experimental program.

Steady-state surface pressures calculated by SOUSSA P1.1 for the three span stations shown in figure 6 are compared with the experimental data in figure 6 for $\alpha=0^\circ$ and in figure 7 for $\alpha = 2^\circ$. The paneling arrays used were 8 by 8, 10 by 10, 12 by 12, and 14 by 14, spaced uniformly both chordwise and spanwise. The curves in figure 6 and 7 show that the pressures obtained with the 8-by-8 array are essentially converged over most of the planform and are in good agreement with experiment (for which the Reynolds number is 9.0×10^6). However, the pressures near the wing edges converge more slowly. Convergence near the edges is improved by use of finer paneling locally (e.g., a cosine distribution, results for which are not shown). The cosine distribution concentrates smaller panels near the edges where pressures usually have the largest gradients.

The calculated pressures in figures 6 and 7 show that immediately ahead of the trailing edge the curves tend to level off as they did for the rectangular wing. This deviation, as mentioned previously, is caused by the condition, still in SOUSSA P1.1, that the average of upper- and lower-surface pressures at the trailing edge is taken to be the value calculated at the center of the upper- and lower-surface panels adjacent to the trailing edge. Also note that in figure 7 the upper-surface and lower-surface pressures do not close at the trailing edge. The failure to close is not a result of the SOUSSA calculation but is caused by the use of cubic-spline curves to connect pressure-values obtained from SOUSSA P1.1.

In addition to the pressures just discussed, the convergence of the integrated pressures (specifically, the lift-curve slope) has also been examined. Reference 4 examined the convergence of integrated aerodynamic forces as a function of the inverse of N, the number of panels in the chordwise or spanwise direction. The variation was found to be essentially linear, giving confidence to linear extrapolation toward estimated converged values for $N \to \infty$. Figure 8 shows a similar plot of the lift-curve slope for the clipped-delta wing as a function of the inverse square root of N_p, the total number of panels in the array, which is an equivalent but more general parameter. The values shown here also lie along an approximately straight line, and the extrapolated estimate of the converged value for $N_p \to \infty$ is indicated. The rate of convergence is independent of angle of attack, and the value of lift-curve slope calculated with the 14-by-14 array (the largest number of panels used for this wing) is about 1.75 percent below the estimated converged value. Inasmuch as integration is a smoothing process, this is not a particularly impressive rate of convergence. In fact, it appears to be slower than the convergence of the pressure over much of the wing. As was mentioned previously, the integration performed in SOUSSA P1.1 to generate generalized aerodynamic forces (such as lift) from the surface pressures is equivalent to rectangular integration. A better integration scheme is obviously needed.

Unsteady pressures have also been measured and calculated (with a uniform 10-by-10 array of panels) for the wing of figure 6 oscillating in pitch about the axis shown. The resulting pressures per unit amplitude of oscillation are compared in figures 9 and 10 for two frequencies. The overall agreement is good. The real component of the pressure is underpredicted a bit over the forward portion of the wing and overpredicted over the aft portion where some boundary-layer thickening probably reduces C_p magnitudes even though the Reynolds number for these tests was 9×10^6 based on average chord. At both frequencies there is some evidence of leading-edge vortex separation at the two outboard stations (Figs. 9 and 10(b) and (c)) which is, of course, not represented in the calculations.

Swept Tapered Wing With and Without Fuselage - Steady-state surface pressures have been calculated by SOUSSA P1.1 for a wing of aspect ratio 4, taper ratio 0.6, quarter-chord sweep angle 45°, and NACA 65A006 airfoil. Calculations have been made for the wing alone with 16 panels spanwise distributed uniformly and 22 panels chordwise also spaced uniformly except for subdivision near the leading edge. Calculations have also been made for the wing with a fuselage (Fig. 11) with a 10-by-10 array of panels distributed uniformly on the wing (200 panels on the half span) and 6 panels circumferentially around the half fuselage with 34 panels distributed somewhat irregularly along its length, as shown in the figure, for a total of 404 panels on the half model. This configuration approximates the wing-body model of reference 7 for which measured pressures are available for comparison. The panel configuration in figure 11 accurately represents the wind-tunnel model except that the paneled fuselage is cylindrical along the length of the wing root, and the tunnel sting is not represented. The cylindrical fuselage section was a restriction imposed by the crude geometry preprocessor that was used to set up these calculations.

Pressures for the wing alone and for the wing of the wing-body combination are compared with experimental values for the wing-body[7] in figure 12 for Mach number 0.6 and angle of attack 4°. The results for the wing of the wing-body combination are in good agreement with the experimental values, and those for the wing alone are in reasonable agreement with experiment outboard, as would be expected. However, the sharp changes and irregular variation of pressure for the wing alone over the subdividied panels near the leading edge illustrate one of the shortcomings of low-order panel methods, that is, sensitivity of the results to paneling geometry. Another illustration of this problem is seen in the calculated distributions of pressure along the fuselage (Fig. 13). In this figure pressures are shown along meridian B, which is 45° off the vertical, and along meridian C which is 75° off the vertical and just above the wing surface (See figure 11). The designations B and C are taken from reference 7. At zero angle of attack, Figure 13(a), the pressures vary smoothly along both meridians and agree well with the experimental data, except toward the aft end of the fuselage where the tunnel sting has not been represented in the present calculations. At 4° angle of attack, figure 13(b), the comparison is still good along meridian B, but on meridian C a large spurious local fluctuation in pressure is calculated adjacent to the wing-root leading edge and trailing edge. Since panel lengths on the fuselage vary substantially in these regions, the calculations were repeated with the two rings of panel nodes marked "r" in figure 11 deleted in order to see if elimination of the short panels adjacent to the leading and trailing edges would help to smooth the fluctuations in pressure. The results are indicated by the diamond symbols in figure 13. Figure 13(b), in particular, shows no improvement in the pressure fluctuations.

From the beginning of the SOUSSA development it was recognized that introduction of higher-order panels (at least linear source and quadratic doublet distributions) would be required to alleviate the kind of problem shown in figure 13(b).

Flutter Calculations for Rectangular Wings

Flutter analysis - Reference 12 reports an experimental flutter investigation of a series of aspect-ratio-5.0 rectangular wings with biconvex (circular arc) airfoils and five thickness ratios, ranging from about 1.4 to 10 percent. Flutter calculations have been made for four of these wings with aerodynamics from SOUSSA P1.1 and from the FAST kernel-function lifting-surface program of reference 11. These Galerkin modal analyses were made with natural modes of a uniform cantilever beam. Three-mode analyses used first and second bending and first torsion modes; five-mode analyses added third bending and second torsion modes. The three-mode and five-mode flutter results are very close together, thereby indicating convergence with respect to the number of modes used.

Convergence Analysis - As a preliminary to the flutter calculations for comparison with the experimental data of reference 12, a study was made of the convergence of the SOUSSA P1.1 aerodynamic forces with respect to the fineness of the paneling. The configuration studied is the rectangular wing of reference 12 with four-percent-thick airfoil. The Mach number is 0.756, and the reduced frequency is 0.114 which is close to the reduced frequency at flutter.

Values of real and imaginary parts of the generalized aerodynamic forces are plotted on the left-hand side of figure 14 as functions of $1/\sqrt{N_p}$ for the first bending mode (modal index 1) and the first torsion mode (index 2). The calculated values shown by the circle symbols are for 8-by-8, 10-by-10, 14-by-14, and 18-by-18 arrays of panels spaced uniformly both chordwise and spanwise. The discontinuities in the ordinate scale should be noted. The solid curves are drawn through the data, and the dashed lines are linear extrapolations from the last calculated points toward estimated converged values for $N_p \to \infty$. For comparison, the square symbols on the ordinate axis indicate values obtained from the FAST subsonic-kernel lifting-surface analysis of reference 11. The latter are not necessarily the values to which the SOUSSA P1.1 results are expected to converge because SOUSSA P1.1 includes airfoil thickness effects, while the lifting-surface analysis does not. These convergence results may be compared with those of reference 10 which show similar trends.

On the right-hand side of the figure are associated values of the flutter-frequency ratio ω/ω_α and the flutter-speed index $V/b\omega_\alpha\sqrt{\mu}$. (Again, note the discontinuity of the ordinate scale). As on the left, the circles and squares indicate SOUSSA and FAST lifting-surface aerodynamics, respectively. The numbers 3 and 5 indicate three-mode and five-mode flutter calculations respectively. The notations 3 x 3 and 6 x 8 indicate the arrangement of downwash collocation points used in the FAST calculations. The two arrangements produced flutter speeds within about one half percent of each other. A further check with 8 x 10 collocation points gave virtually identical results to those of the 6 x 8, and therefore the results are judged to be converged with respect to the number of collocation points.

An examination of the real and imaginary parts of A_{22}, the weighted twisting moment due to first-torsion-mode motion, shows two counteracting effects as the number of panels increases. The real part of A_{22} is positive and increasing, indicating an increasing divergent moment that tends to decrease the flutter speed. In contrast, the imaginary part of A_{22} is negative and becoming more negative. This increase in damping of the first-torsion mode tends to increase the flutter speed. The net effect is less than one percent decrease of the flutter-speed index as paneling increased from 10-by-10 to 18-by-18. Although this change is small, the indicated trend would bring SOUSSA P1.1 results even closer to the lifting-surface values if the number of panels were increased further.

Comparison with Experiment - In view of the results of the convergence analysis, the SOUSSA P1.1 calculations made for comparison with the experimental flutter data of reference 12 employed a uniform 18-by-18 array of panels and five vibration modes. The corresponding FAST kernel-function calculations also employed five vibration modes, and the downwash collocation points were arrayed six chordwise by eight spanwise at the program-default locations.

The flutter speeds calculated by the two methods for the four-percent-thick wing (Fig. 15) are close together, and both closely follow the experimental trend with Mach number. However, they are 10 to 11 percent unconservative at the lower Mach numbers up to as much as 14 percent unconservative at Mach numbers near 0.9. The flutter frequencies calculated by both methods, on the other hand, are very close to the experimental values.

Figure 16 shows measured[12] and calculated flutter-speed-index values for four different wing thicknesses -- 1.4, 4, 6, and 10 percent. The two curves for the four-percent-thick wing are repeated from figure 15. The solid circles for 1.4-percent thickness are slightly below the solid squares, and the 6- and 10-percent thick results are slightly above, thereby showing a small but monotonic effect of thickness. The FAST results, of course, contain no aerodynamic effects of airfoil thickness. Consequently, the differences between FAST results for the different wing thicknesses are caused entirely by differences in model mass, stiffness, and structural-damping properties. Hence the calculated aerodynamic effects of thickness at a given Mach number are perhaps best assessed by comparing the SOUSSA calculations with FAST results for the same wing thickness. The FAST-SOUSSA differences here range from about one percent for the 1.4-percent-thick wing to about five percent for the 10-percent-thick wing. These differences are small, and the trend indicated cannot be confirmed by the measured data because of the experimental scatter.

The new kernel-function results shown in figures 15 and 16 do not agree with the kernel-function-derived results shown on figure 5 of reference 12 which showed close agreement with the experiments. The current FAST program is believed to be numerically superior to the kernel-function program of 1959, and to yield a more accurate lifting-surface results. Some of the improvements in FAST relative to its predecessors are discussed in reference 18.

A possible explanation of the experimental flutter speeds being lower than the calculated values is as follows: For thin wings with sharp leading edges it has been observed experimentally that, even at small (nonzero) angles of attack (static or dynamic), a localized leading edge flow-separation "bubble" occurs. (See also the discussion of figure 4(b) above). The bubble increases the divergent twisting moment above that which would be indicated by attached-flow theory. Such an increased moment acts to lower the flutter speed. Consequently, it is possible that the measured flutter speeds for the rectangular wings of figures 15 and 16 and reference 12 are lower than those that would be calculated by any attached-flow theory.

Concluding Remarks

Although the SOUSSA method has the ability to handle bodies having arbitrary shapes, motions, and deformations, the present study has focused on applications to some simple wings in steady and unsteady motion, including flutter, in order to assess the validity, accuracy, and usefulness of the current SOUSSA P1.1 program by comparison of results with those of lifting-surface theory and existing experimental data. SOUSSA P1.1 results are found to be very close to those obtained from steady and unsteady lifting-surface theory and to agree satisfactorily with experiment for conditions where agreement should be expected.

In addition, the results and experience with the program serve to highlight and quantify needed improvements which had already been recognized. These include use of higher-order panels (first-order source, secondorder doublet), improved implementation of Kutta condition, elimination of the SPAR data base and data handling utilities, and (based on operations count) transposition and revision of the solution algorithm. For moderate to large problems (a few hundred to many hundreds of panels) these changes should reduce the cost of a converged solution by nearly an order of magnitude.

References

[1] Morino, Luigi: A General Theory of Unsteady Compressible Potential Aerodynamics. NASA CR-2464, 1974.

[2] Morino, Luigi; and Tseng, Kadin: Time-Domain Green's Function Method for Three-Dimensional Nonlinear Subsonic Flows. AIAA Paper 78-1204, 1978.

[3] Morino, Luigi: Steady, Oscillatory, and Unsteady Subsonic and Supersonic Aerodynamics - Production Version (SOUSSA P1.1) - Vol. I, Theoretical Manual. NASA CR 159130, 1980.

[4] Smolka, Scott A.; Preuss, Robert D.; Tseng, Kadin; and Morino, Luigi: Steady, Oscillatory, and Unsteady Subsonic and Supersonic Aerodynamics - Production Version 1.1 (SOUSSA P1.1), Vol. II - User/Programmer Manual. NASA CR 159131, 1980.

[5] Lessing, Henry C.; Troutman, John L.; and Menees, Gene P.: Experimental Determination of the Pressure Distribution on a Rectangular Wing Oscillating in the First Bending Mode for Mach Numbers from 0.24 to 1.30. NASA TN D-344, 1960.

[6] Hess, R. W.; Wynne, E. C.; and Cazier, F. W.: Static and Unsteady Pressure Measurements on a 50 Degree Clipped Delta Wing at M = 0.9. AIAA Paper 82-0686-CP, 1982.

[7] Loving, Donald L.; and Estabrooks, Bruce B.: Transonic-Wing Investigation in the Langley 8-Foot High-Speed Tunnel at High Subsonic Mach Numbers and at a Mach Number of 1.2. NACA RM L51F07, 1951.

[8] Rowe, W. S.; Redman, M. C.; Ehlers, F. E.; and Sebastian, J. D.: Prediction of Unsteady Aerodynamic Loadings Caused by Leading Edge and Trailing Edge Control Surface Motions in Subsonic Compressible Flow - Analysis and Results. NASA CR-2543, 1975.

[9] Rowe, W. S; Sebastian, J. D.; and Petrarca, J. R.: Reduction of Computer Usage Costs in Predicting Unsteady Aerodynamic Loadings Caused by Control Surface Motions. NASA CR-3009, 1979.

[10] Rowe, W. S.; and Cunningham, H. J.: On the Convergence of Unsteady Generalized Aerodynamic Forces. AIAA Paper 81-0647, 1981.

[11] Desmarais, Robert N.; and Bennett, Robert M.: User's Guide for a Modular Flutter Analysis Software System (FAST Version 1.0). NASA Technical Memorandum 78720, 1978.

[12] Doggett, Robert V., Jr.; Rainey, A. Gerald; and Morgan, Homer G.: An Experimental Investigation of Aerodynamic Effects of Airfoil Thickness on Transonic Flutter Characteristics. NASA TM X-79, 1959.

[13] Morino, Luigi; and Chen, Lee-Tzong: Indicial Compressible Potential Aerodynamics Around Complex Aircraft Configurations. In "Aerodynamic Analyses Requiring Advanced Computers." NASA SP-347, Part II. pp. 1067-1110, 1975.

[14] Giles, G. L.; and Haftka, R. T.: SPAR Data Handling Utilities. NASA TM-78701, 1978.

[15] Magnus, Alfred E.; and Epton, Michael E.: PAN AIR - A Computer Program for Predicting Subsonic or Supersonic Linear Potential Flows about Arbitrary Configurations Using a Higher Order Panel Method. Volume I - Theory Document. NASA CR 3251, 1980.

[16] Sidwell, Kenneth W.; Baruah, Pranab K.; and Bussoletti, John E.: PAN AIR - A Computer Program for Predicting Subsonic or Supersonic Linear Potential Flows about Arbitrary Configurations Using a Higher Order Panel Method. Volume II - User's Manual. NASA CR 3252, 1980.

[17] Watkins, Charles E.; Runyan, Harry L.; and Woolston, Donald S.: On the Kernel Function of the Integral Equation Relating the Lift and Downwash Distributions of Oscillating Finite Wings in Subsonic Flow. NACA Rep. 1234, 1955.

[18] Desmarais, Robert N.: An Accurate Method for Evaluating the Kernel of the Integral Equation Relating Lift to Downwash in Unsteady Potential Flow. AIAA Paper 82-0687, 1982.

[19] Maskew, Brian: Prediction of Subsonic Aerodynamic Characteristics: A Case for Low-Order Panel Methods. Journal of Aircraft, Vol. 19, No. 2, Feb. 1982.

[20] Guruswamy, P.; and Goorjian, P. M.: Comparisons Between Computations and Experimental Data in Unsteady 3D Transonic Aerodynamics, Including Aeroelastic Applications. AIAA Paper No. 82-0690-CP, 1982.

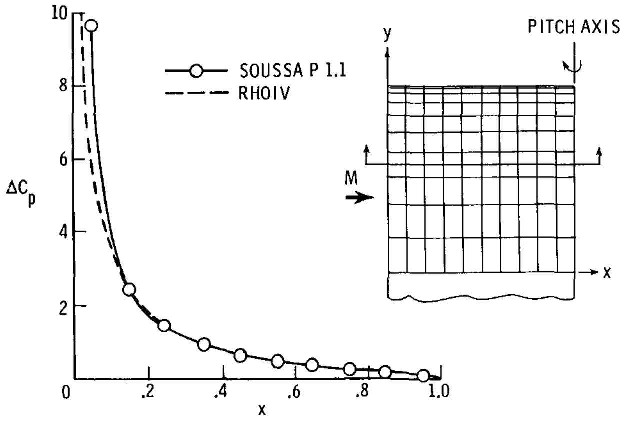

(a) k = 0.0

Fig. 1 Calculated lifting-pressure distributions for aspect-ratio-2 rectangular wing pitching about trailing edge. M = 0.9, y = 0.575.

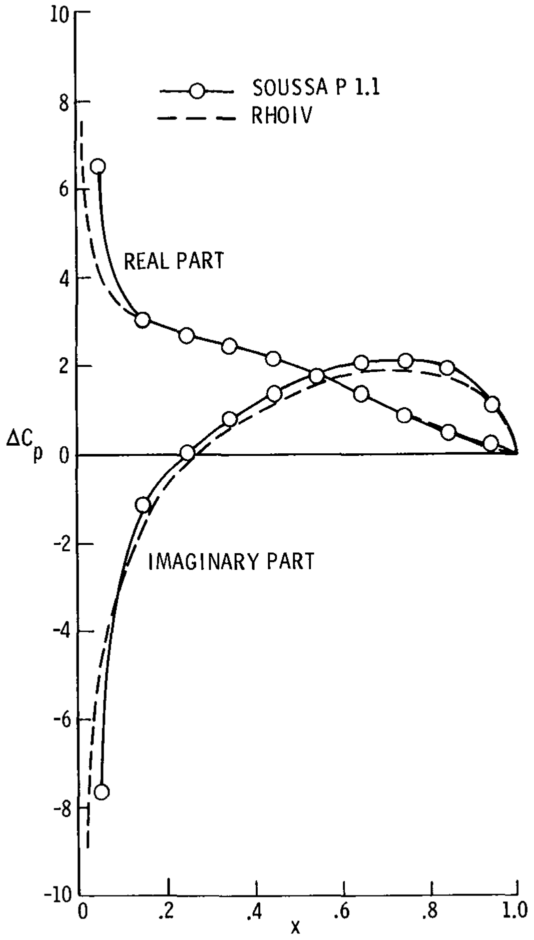

(b) k = 0.3

Fig. 1 Concluded.

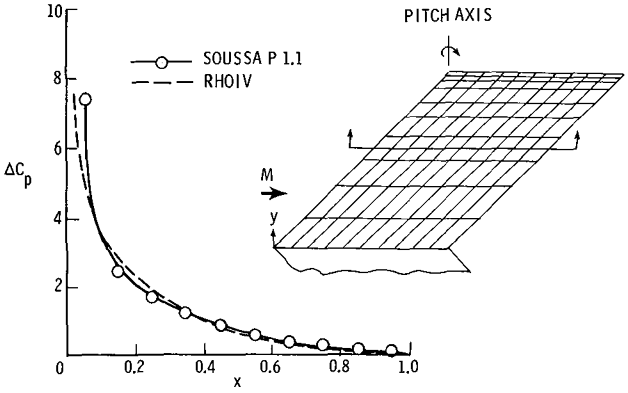

(a) k = 0.0

Fig. 2 Calculated lifting-pressure distributions for aspect-ratio-2, 45-degree-swept wing pitching about root trailing edge. M = 0.9, y = 0.575.

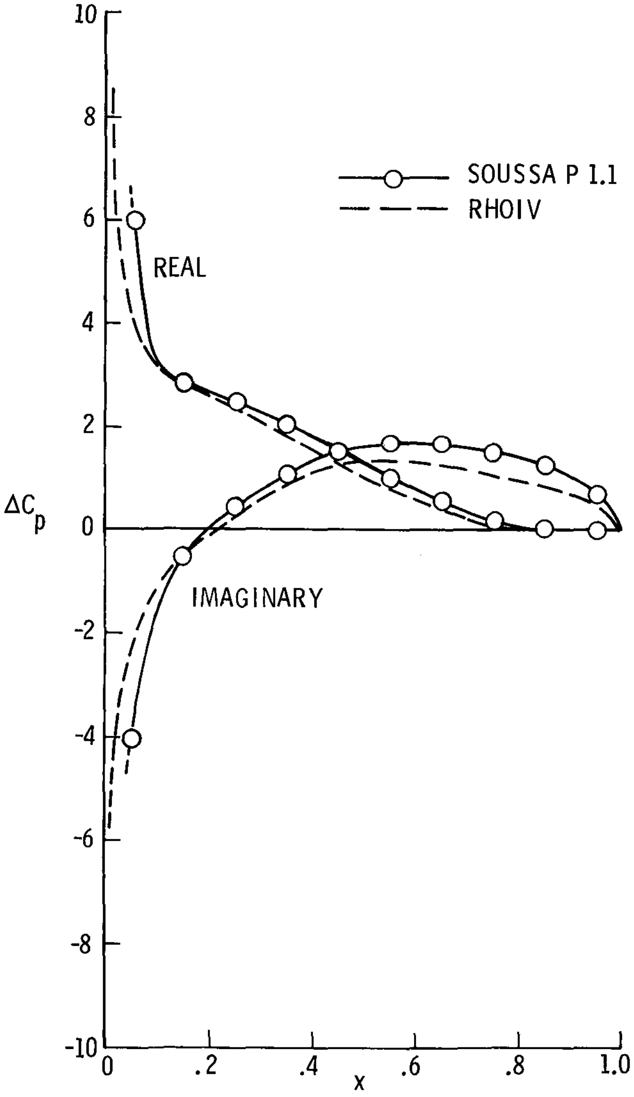

(b) k = 0.3

Fig. 2 Concluded.

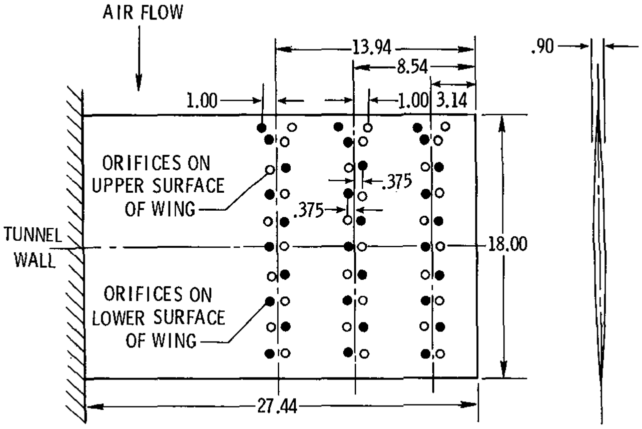
AIR FLOW
13.94
8.54
.90
1.00
1.00
3.14
ORIFICES ON UPPER SURFACE OF WING
.375
.375
TUNNEL WALL
18.00
ORIFICES ON LOWER SURFACE OF WING
27.44

Fig. 3 Rectangular wing model of reference 5. All dimensions are in inches.

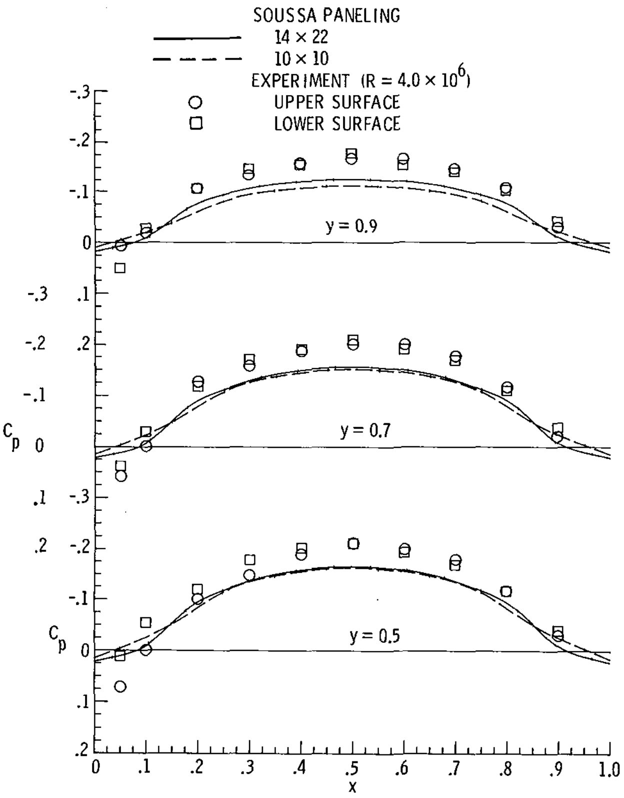

(a) α = 0°.

Fig. 4 Steady-state pressure distributions on aspect-ratio-3 rectangular wing at M = 0.70.

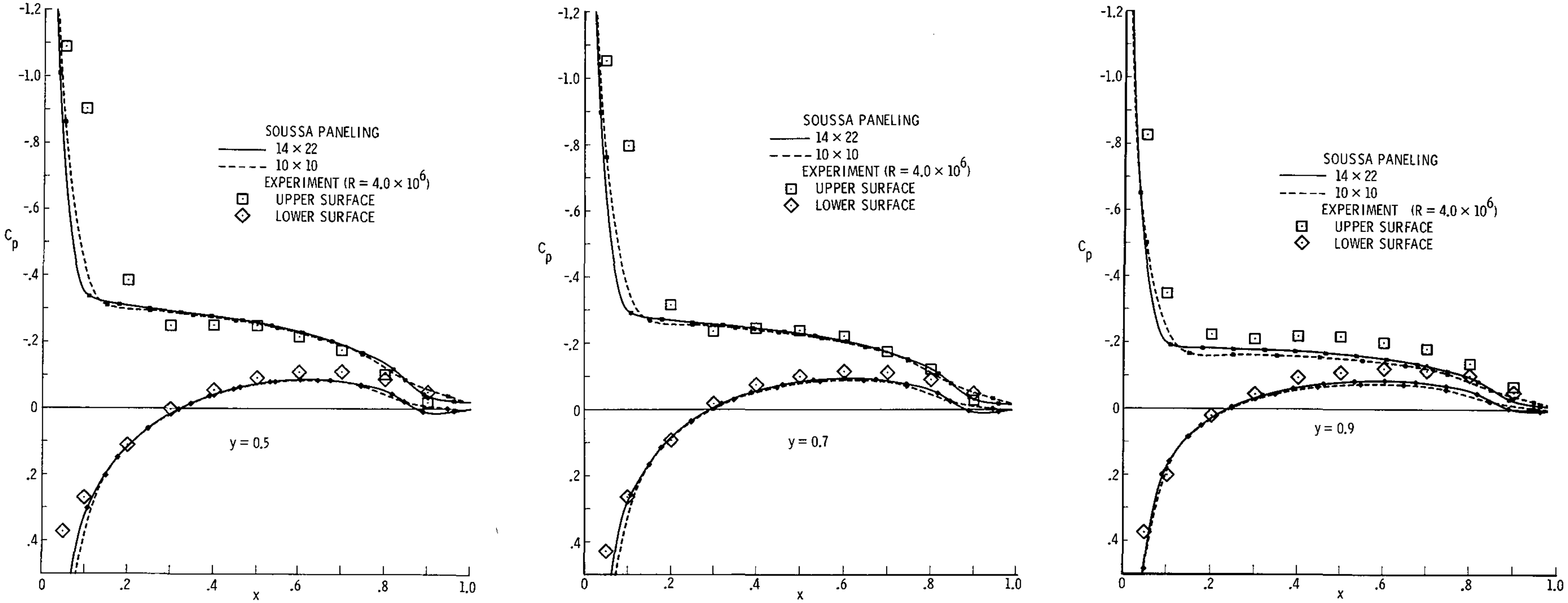

(b) α = 5°

Fig. 4 Concluded.

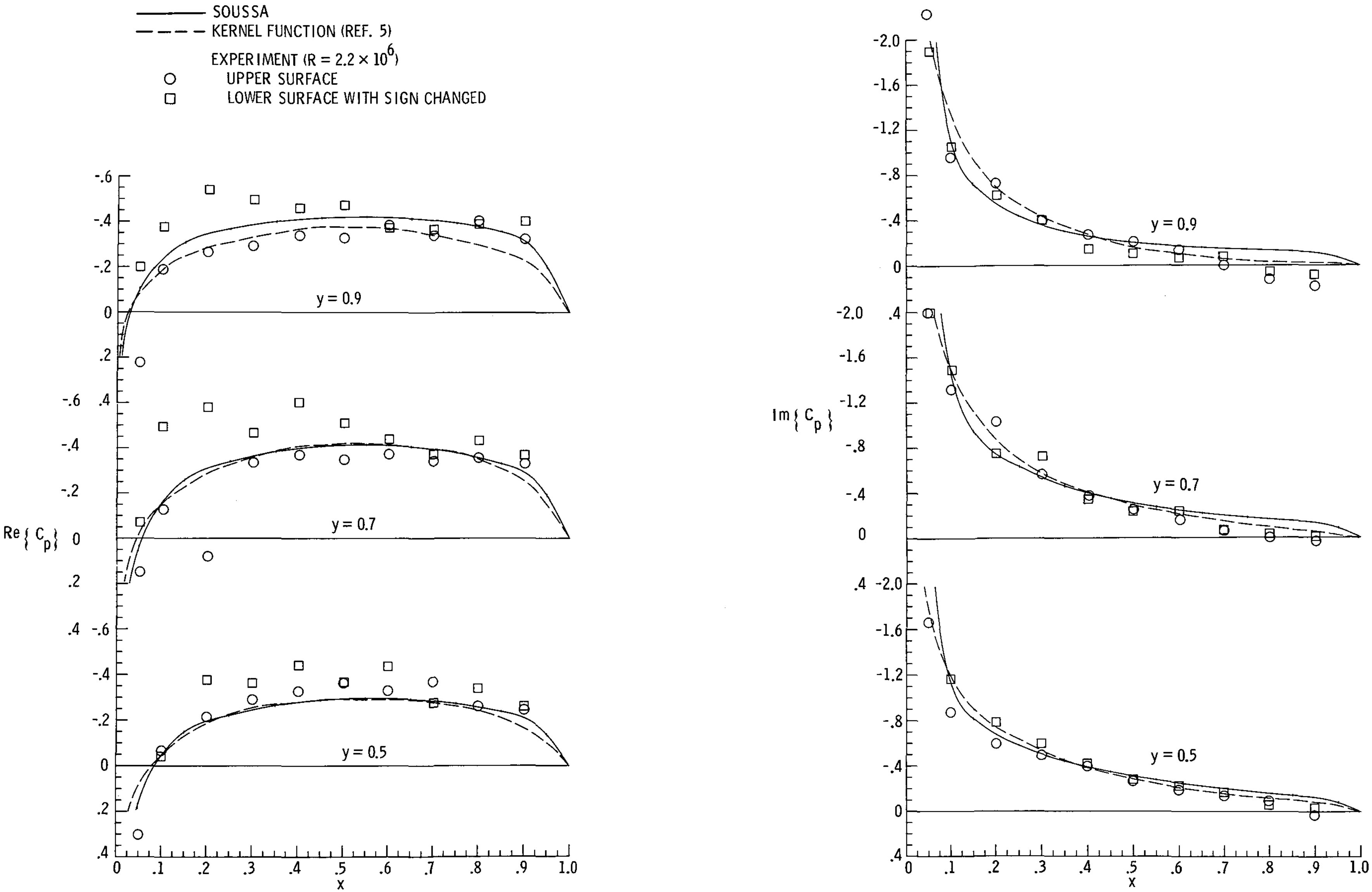

Fig. 5 Unsteady pressures on aspect-ratio-3 rectangular wing at $\alpha = 0^{o}$. M = 0.24, k = 0.47.

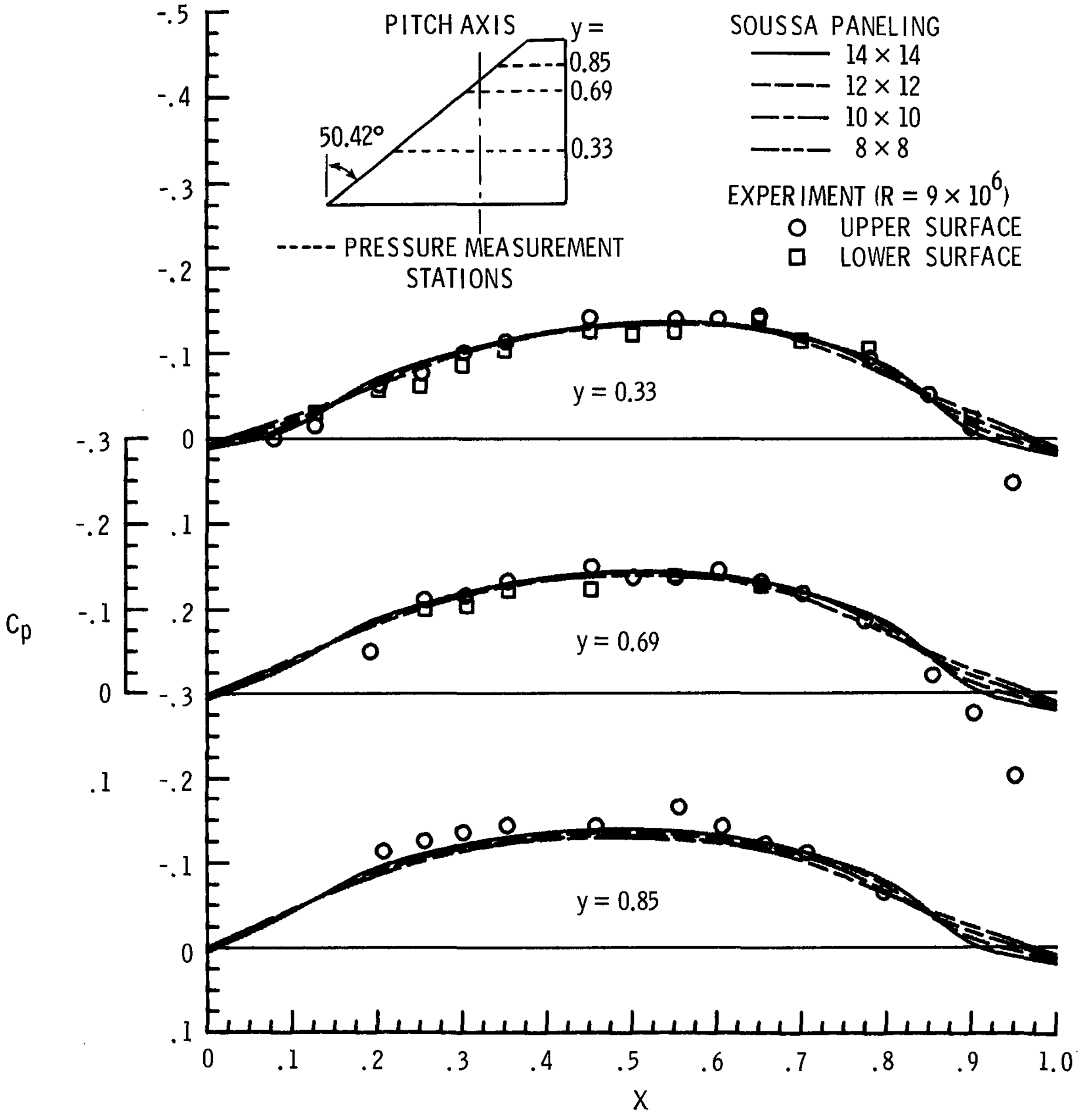

Fig. 6 Steady-state surface pressure on clipped-tip delta wing. M = 0.40, $\alpha = 0^{\circ}$.

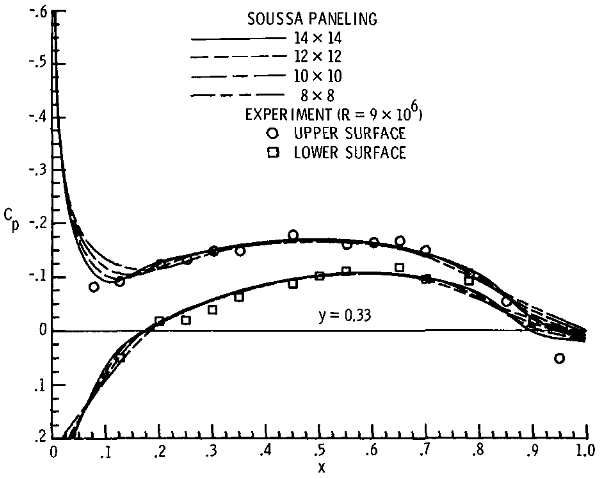

(a) y = 0.33

Fig. 7 Steady-state surface pressures on clipped-tip delta wing. M = 0.40, $\alpha = 2^{o}$.

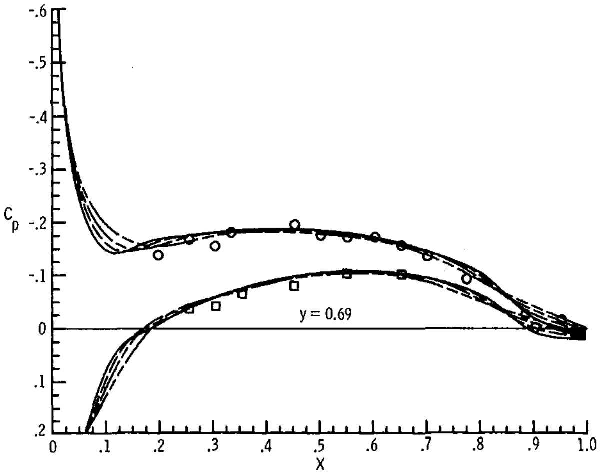

(b) y = 0.69

Fig. 7 Continued.

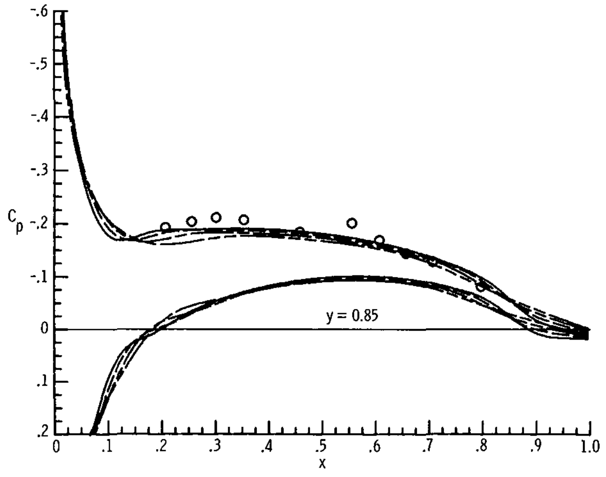

(c) y = 0.85

Fig. 7 Concluded.

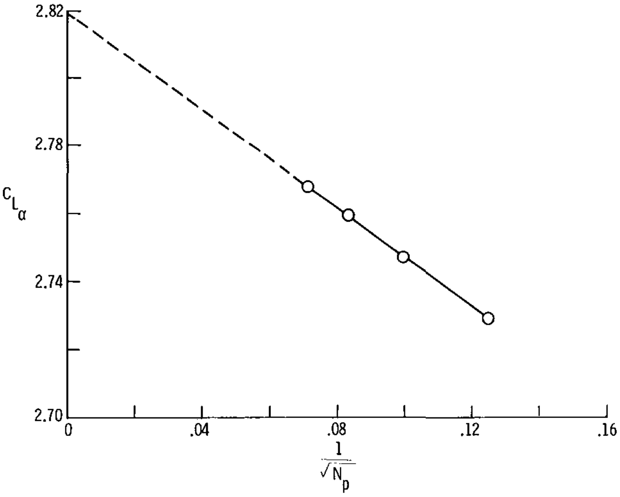

Fig. 8 Paneling convergence of lift-curve slope for clipped-tip delta wing. M = 0.40.

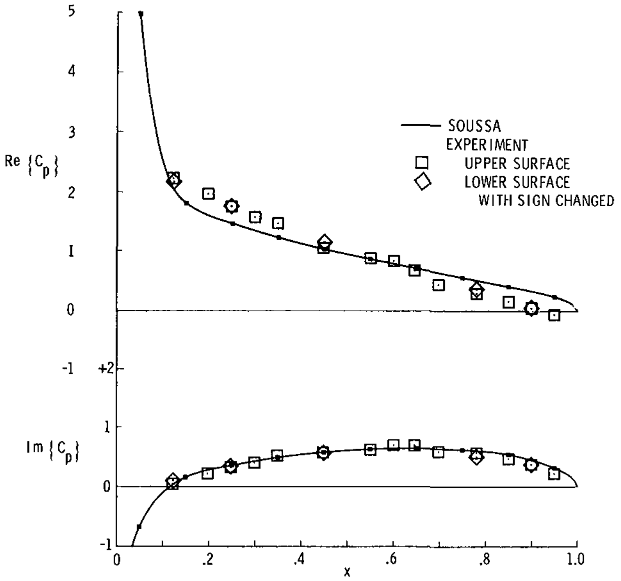

(a) y = 0.33

Fig. 9 Surface pressures on clipped-tip delta wing oscillating in pitch. M = 0.40, k = 0.33.

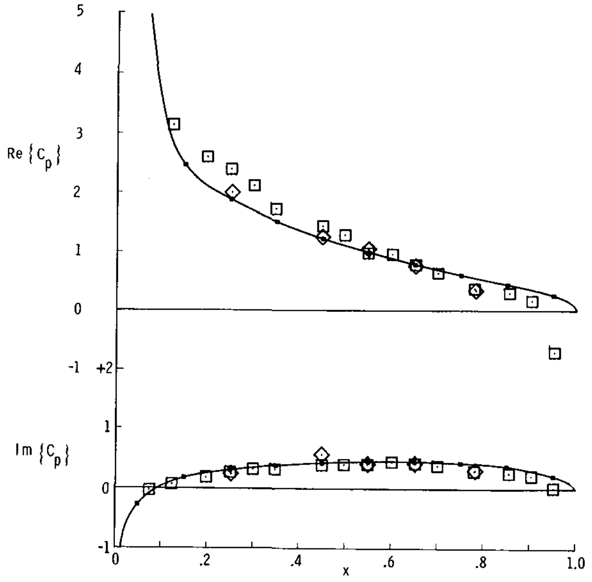

(b) y = 0.69

Fig. 9 Continued.

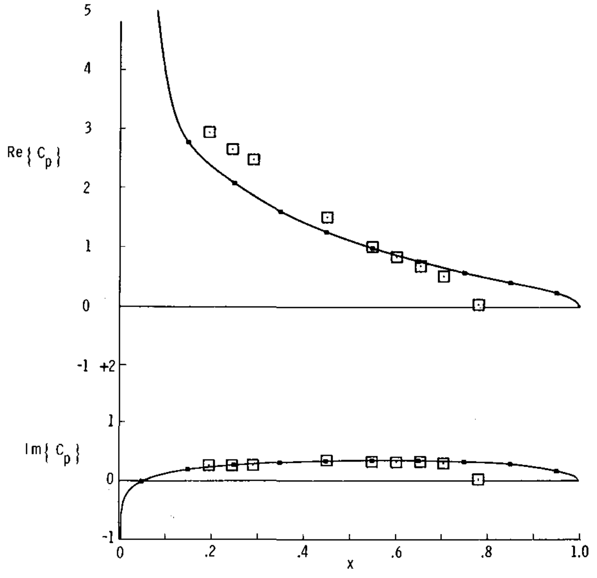

(c) y = 0.85

Fig. 9 Concluded.

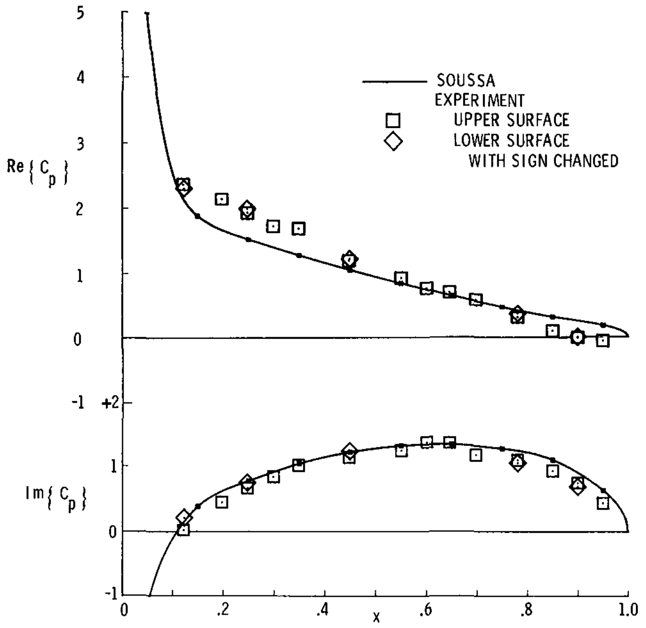

(a) y = 0.33

Fig. 10 Surface pressures on clipped-tip delta wing oscillating in pitch. M = 0.40, k = 0.66.

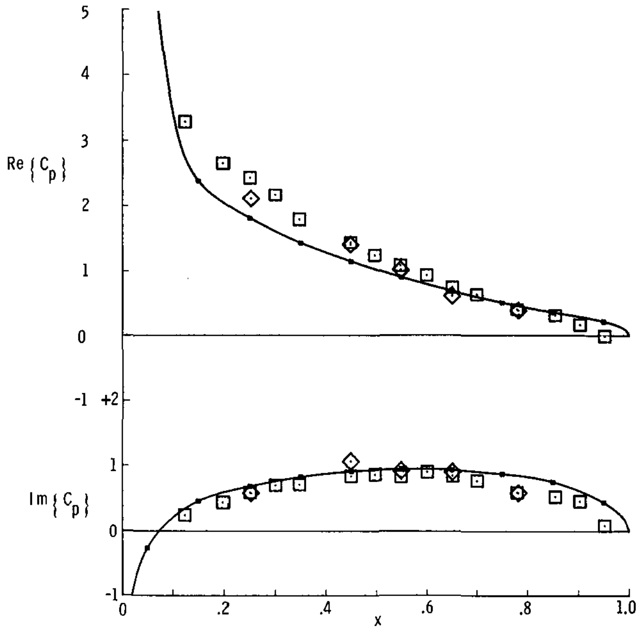

(b) y = 0.69

Fig. 10 Continued

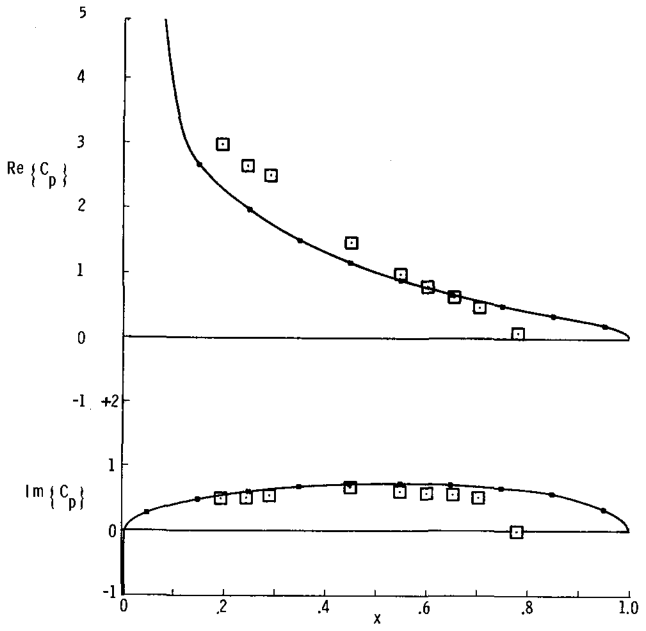

(c) y = 0.85

Fig. 10 Concluded.

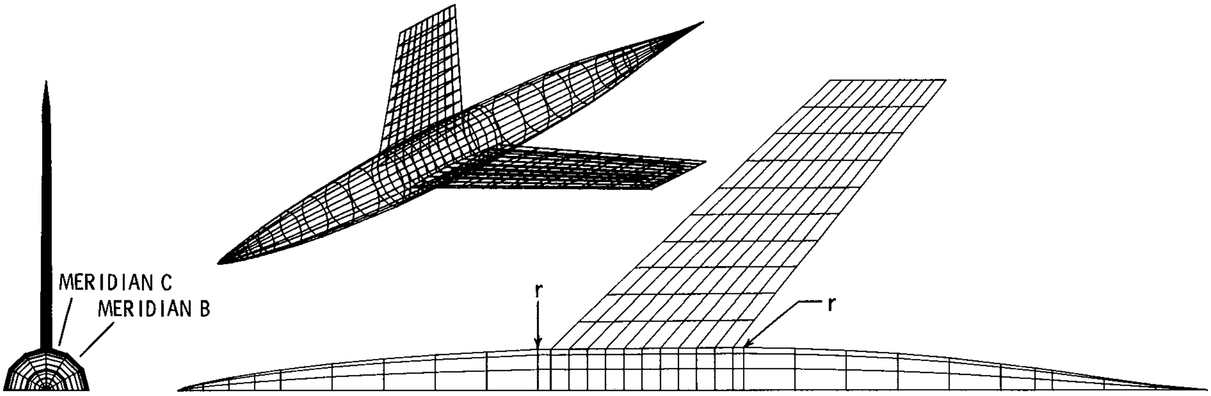
MERIDIAN C
MERIDIAN B
r
r

Fig. 11 SOUSSA paneling for model of reference 7.

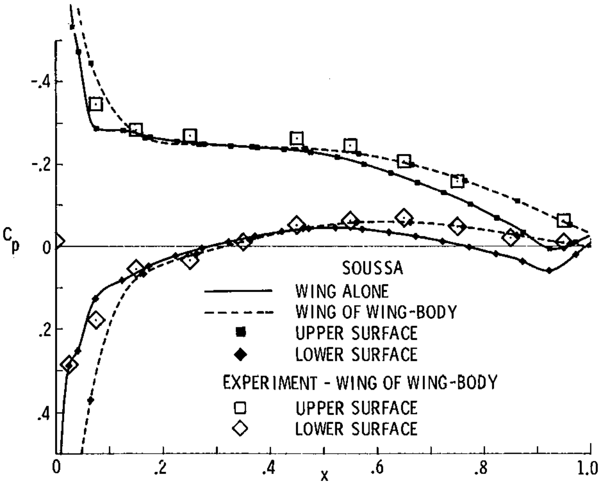

(a) y = 0.20

Fig. 12 Calculated and measured surface pressures on wing of wing-body configuration. $M = 0.6$, $\alpha = 4^{\circ}$.

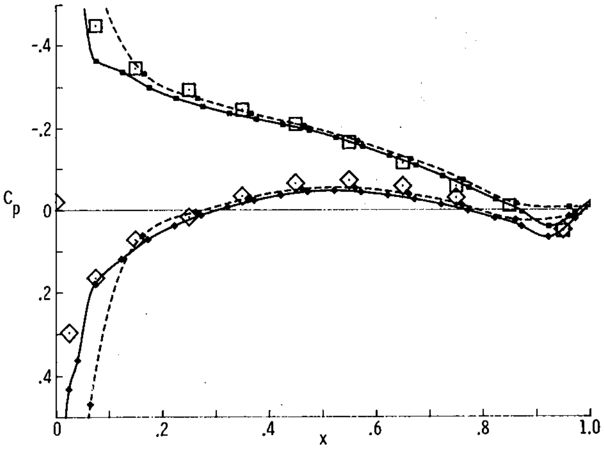

(b) y = 0.80

Fig. 12 Concluded

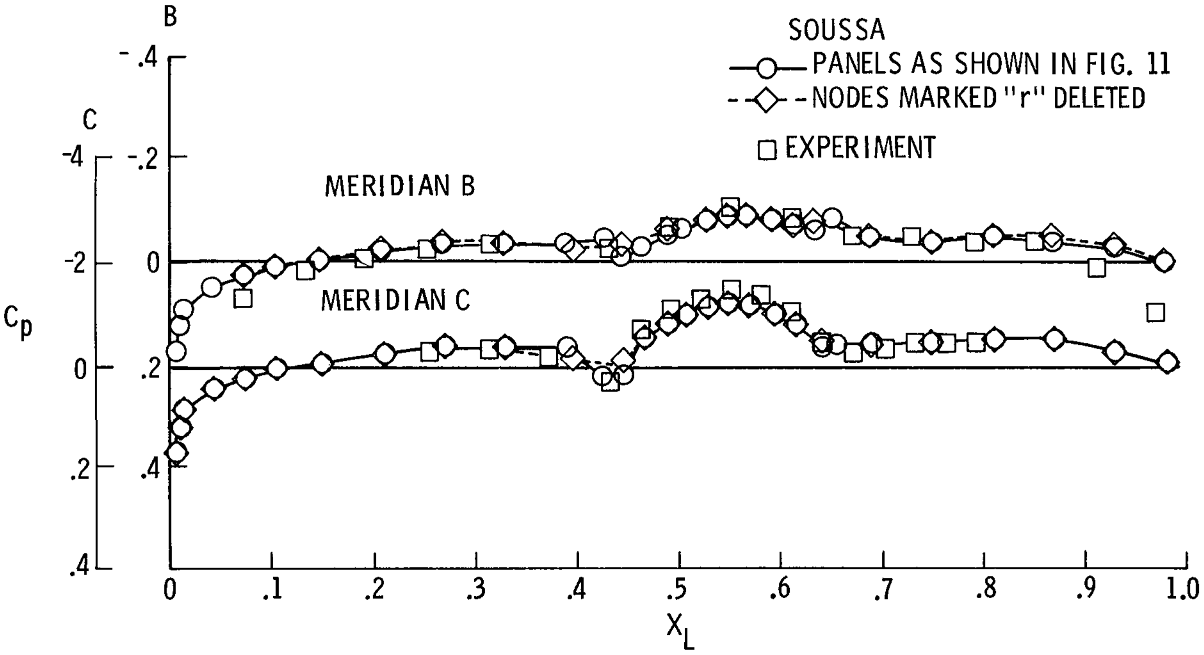

(a) $\alpha = 0^o$

Fig. 13 Calculated and measured surface pressures on fuselage of wing-body configuration. M = 0.6.

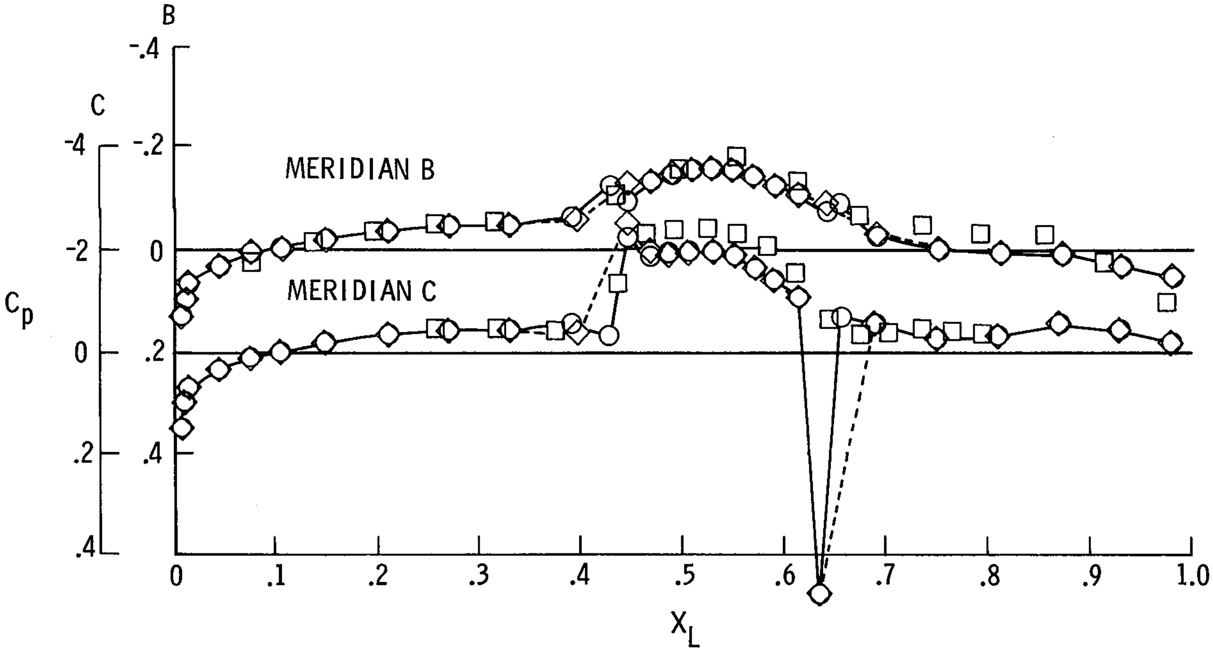

(b) $\alpha = 4^o$

Fig. 13 Concluded.

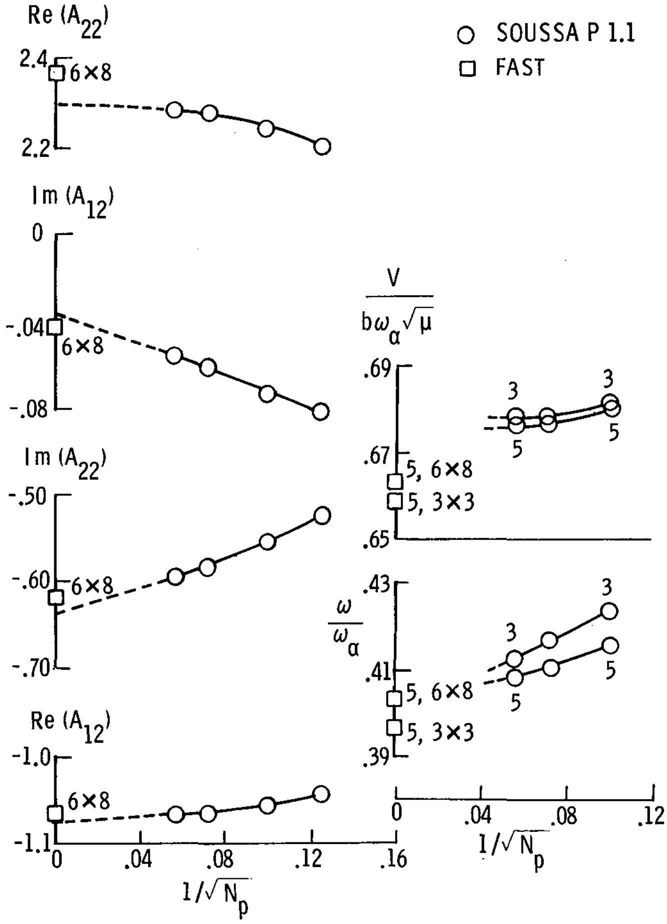

Fig. 14 Paneling convergence of generalized aerodynamic forces and flutter characteristics for four-percent-thick rectangular wing of reference 12. M = 0.756.

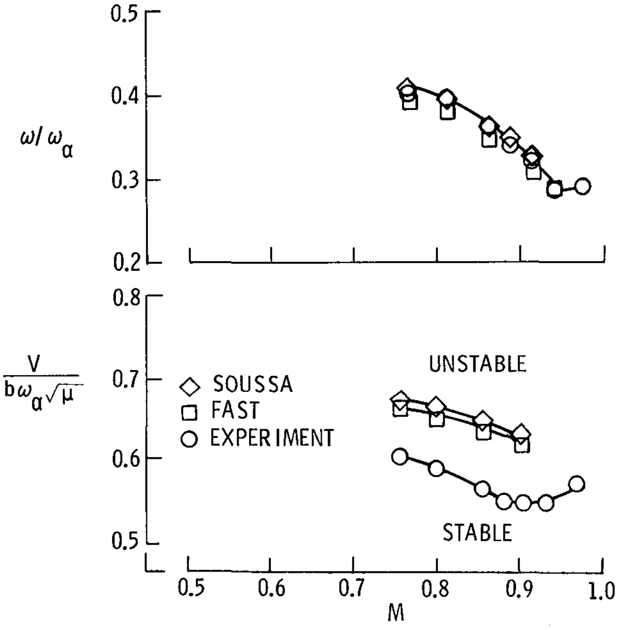

Fig. 15 Flutter characteristics for four-percent-thick rectangular wing of reference 12.

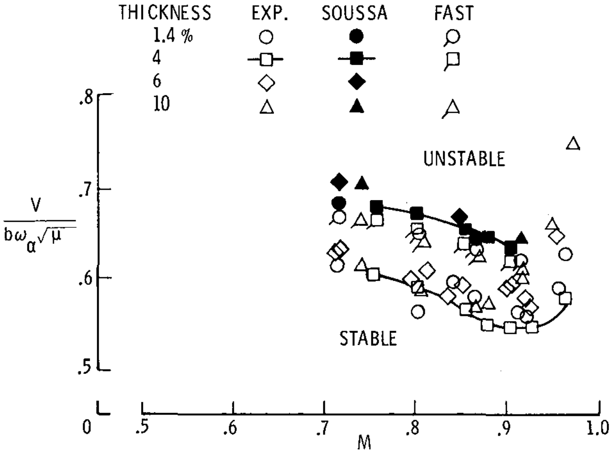

Fig. 16 Effect of thickness on flutter-speed-index for the rectangular wings of reference 12.

1. Report No. NASA TM 84485	2. Government Accession No.	3. Recipient's Catalog No.

4. Title and Subtitle
Subsonic Aerodynamic and Flutter Characteristics of Several Wings Calculated by the SOUSSA P1.1 Panel Method

5. Report Date
May 1982

6. Performing Organization Code
505-33-53-07

7. Author(s)
E. Carson Yates, Jr., Herbert J. Cunningham, Robert N. Desmarais, Walter A. Silva, and Bohdan Drobenko

8. Performing Organization Report No.

9. Performing Organization Name and Address

NASA Langley Research Center
Hampton, VA 23665

10. Work Unit No.

11. Contract or Grant No.

12. Sponsoring Agency Name and Address
National Aeronautics and Space Administration
Washington, DC 20546

13. Type of Report and Period Covered
Technical Memorandum

14. Sponsoring Agency Code

15. Supplementary Notes

Presented as AIAA Paper No. 82-0727 at the AIAA/ASME/ASCE/AHS 23rd Structures, Structural Dynamics and Materials Conference, New Orleans, LA, May 10-12, 1982.

16. Abstract

The SOUSSA (Steady, Oscillatory, and Unsteady Subsonic and Supersonic Aerodynamics) program is the computational implementation of a general potential-flow analysis (by the Green's function method) that can generate pressure distributions on complete aircraft having arbitrary shapes, motions, and deformations. This paper presents results of some applications of the initial release version of this program to several wings in steady and oscillatory motion, including flutter. The results are validated by comparisons with other calculations and experiments. Experiences in using the program as well as some recent improvements are described.

17. Key Words (Suggested by Author(s)) Unsteady Aerodynamics Panel Methods Potential Flow Aeroelasticity	18. Distribution Statement Unclassified Unlimited Subject Category - 02

19. Security Classif. (of this report) Unclassified	20. Security Classif. (of this page) Unclassified	21. No. of Pages 20	22. Price A02

For sale by the National Technical Information Service, Springfield, Virginia 22161

LANGLEY RESEARCH CENTER
3 1176 00503 4179